The comparisons show that the imperfect gas effects are about 5% for very strong shock waves ($M_S \sim 20$) into air at one atmosphere pressure, whereas, for strong shock waves ($M_S \sim 10$) into 2.63 atm, the effects are about 7%. These effects are, of course, maximum at highest density and therefore behind the reflected shock wave and at other stagnation conditions. For high pressure or high density shock tube studies, the results of Lewis and Burgess[1, 2] are to be preferred over the previously published perfect gas results.

References

[1] Lewis, C. H. and Burgess, E. G., III, "Charts of normal shock wave properties in imperfect air," Arnold Engineering Development Center-TDR-64-43 (1964).

[2] Lewis, C. H. and Burgess, E. G., III, "Charts of normal shock wave properties in imperfect nitrogen," Arnold Engineering Development Center-TDR-64-104 (1964).

[3] Lewis, C. H. and Neel, C. A., "Thermodynamic properties for imperfect air and nitrogen to 15,000°K," AIAA J. 2, 1847–1849 (1964).

[4] Neel, C. A. and Lewis, C. H., "Interpolations of imperfect air thermodynamic data I. At constant entropy," Arnold Engineering Development Center-TDR-64-183 (1964).

[5] Neel, C. A. and Lewis, C. H., "Interpolations of imperfect air thermodynamic data II. At constant pressure," Arnold Engineering Development Center-TDR-64-184 (1964).

[6] Neel, C. A. and Lewis, C. H., "Interpolations of imperfect nitrogen thermodynamic data I. At constant entropy," Arnold Engineering Development Center-TDR-64-212 (1964).

[7] Neel, C. A. and Lewis, C. H., "Interpolations of imperfect nitrogen thermodynamic data II. At constant pressure," Arnold Engineering Development Center-TDR-64-213 (1964).

[8] Feldman, S., "Hypersonic gas dynamic charts for equilibrium air," Avco Research Rept. 40 (1957).

[9] Bernstein, L., "Tabulated solutions of the equilibrium gas properties behind the incident and reflected normal shock-wave in a shock tube. I-nitrogen; II-oxygen," Aeronautical Research Council Rept. 22, 778 (1961).

Effects of Diffusion in Laminar Hypersonic Wakes

J. J. KANE*

Aerospace Corporation, San Bernardino, Calif.

Introduction

DIFFUSION in laminar boundary layers has been shown[1] to reduce peak electron concentration levels by two orders of magnitude. It is the purpose of this note to describe such effects for laminar wakes since the electron densities that are generated there may, when carried into the turbulent wake, determine the observable signature of a re-entry vehicle.

Basic Equations and Solutions

The ionization due to sodium as a trace contaminant is considered. It is assumed that the presence of the sodium has no significant effect on local velocity and enthalpy, which are then described in the same manner as for the clean wake.[2] It is also assumed that the ionization reaction is far from equilibrium so that only the forward reaction is considered. To determine the sodium ion distribution, therefore, only the species equation need be considered.

For binary diffusion with constant Schmidt number in axisymmetric flow, the conservation of species for small r is[3]

$$U\frac{\partial C}{\partial x} = 2D\frac{\partial^2 C}{\partial r^2} + \frac{\dot{w}}{\rho} \tag{1}$$

Received October 29, 1964.

* Member of the Technical Staff, Technology Division. Member AIAA.

For a near wake analysis, it has been shown[2] that the wake centerline velocity can be adequately described by

$$\frac{U_0}{U_e} = \left\{\frac{4\pi\mu_0 U_e x}{3D_f}\right\}^{1/2} \tag{2}$$

where D_f = frictional drag. Equation (2) is valid only up to values of U_0/U_e of roughly 0.5. The results of this note are carried only this far.

Letting the velocity for small r be represented by the centerline velocity, the conservation of species becomes

$$Ax^{1/2}(\partial C/\partial x) = 2D(\partial^2 C/\partial r^2) + (\dot{w}/\rho) \tag{3}$$

where

$$A = U_e\{4\pi\mu_0 U_e/3D_f\}^{1/2} \tag{4}$$

The boundary conditions are

$$x = 0 : C = C_0(r) \tag{5}$$

$$r = 0 : \partial C/\partial r = 0 \tag{6}$$

$$r = \infty : C = 0 \tag{7}$$

Introducing the variable t, where

$$t = x^{1/2} \tag{8}$$

Eq. (3) becomes

$$\frac{A}{2}\frac{\partial C}{\partial t} = 2D\frac{\partial^2 C}{\partial r^2} + \frac{\dot{w}}{\rho} \tag{9}$$

The source term for the reactions considered is proportional to concentrations of species which scale with some power of x.

It is therefore reasonable to represent the source term as

$$\dot{w}/\rho = W_0 t^{2n} g(r) \tag{10}$$

where W_0 and n are constants. The function $g(r)$ includes in the radial variation of ion production, the radial variation of species profiles, and temperature. In this study, $g(r)$ was taken to be the same type of function as $C_0(r)$. The constant W_0 depends on the temperature, which is approximately constant along the near wake centerline.[2] Solutions were obtained to Eq. (9) for three types of initial profile, $C_0(r)$.

Exponential Profiles

If the initial ion profile and $g(r)$ are represented by

$$C_0(r) = C_0 e^{-r/B} \tag{11}$$

$$g(r) = e^{-r/V} \tag{12}$$

where C_0 is a constant, then the solution to Eq. (9) is

$$C(r,t) = \frac{C_0}{2} e^{4Dt/B^2A}\left\{e^{-r/B}\left[2 - \operatorname{erfc}\left(\frac{r}{2}\left[\frac{A}{4Dt}\right]^{1/2} - \left[\frac{4Dt}{B^2A}\right]^{1/2}\right)\right] + e^{r/B}\operatorname{erfc}\left(\left[\frac{4Dt}{B^2A}\right]^{1/2} + \frac{r}{2}\left[\frac{A}{4Dt}\right]^{1/2}\right)\right\} + \frac{e^{-r/V}2W_0(2n)!}{A}\int_0^t \ldots 2n + 1 \ldots \int_0^t e^{4Dt/V^2A}\, dt^{2n+1} - \frac{W_0}{A}(2n)!\int_0^t \ldots 2n + 1 \ldots \int_0^t e^{-r/V}\, e^{4Dt/V^2A}\operatorname{erfc}\left\{-\left[\frac{4Dt}{V^2A}\right]^{1/2} + \frac{r}{2}\left[\frac{A}{4Dt}\right]^{1/2}\right\} dt^{2n+1} + \frac{W_0(2n)!}{A}\int_0^t \ldots 2n + 1 \ldots \int_0^t e^{r/V}\, e^{4Dt/V^2A}\operatorname{erfc}\left\{\left[\frac{4Dt}{V^2A}\right]^{1/2} + \frac{r}{2}\left[\frac{A}{4Dt}\right]^{1/2}\right\} dt^{2n+1} \tag{13}$$

For the ion mass fraction along the wake centerline ($r = 0$),

$$C(0, t) = C_0 e^{4Dt/B^2A} \operatorname{erfc}\left[\frac{4Dt}{B^2A}^1\right]^{1/2} + \frac{2W_0(2n)!}{A} \int_0^t \cdots 2n+1 \cdots \int_0^t e^{4Dt/V^2A} \times \operatorname{erfc}\left[\frac{4Dt}{V^2A}\right]^{1/2} dt^{2n+1} \quad (14)$$

where

$$\int_0^t \cdots 2n+1 \cdots \int_0^t dt^{2n+1}$$

designates successive integration $2n + 1$ times.

Parabolic Profiles

If the initial ion profile and $g(r)$ are represented by

$$C_0(r) = C_0[1 - (r/B)^2] \quad (15)$$

$$g(r) = 1 - (r/V)^2 \quad (16)$$

and the boundary condition (7) changed to apply at $r = B$ and V rather than at $r = \infty$, then the solution to Eq. (9) is

$$C(r,t) = \frac{2W_0}{A}\left\{1 - \frac{r^2}{V^2}\right\}\frac{t^{2n+1}}{(2n+1)} + \frac{64W_0(2n)!}{A\pi^3}\sum_{m=1}^{\infty}\frac{(-1)^{m+1}}{(2m-1)^3}\left[\cos(2m-1)\frac{\pi r}{2V}\right] \times \left\{\int_0^t \cdots 2n+1 \cdots \int_0^t \exp -\frac{(2m-1)^2\pi^2 tD}{V^2A} \times dt^{2n+1} - \frac{t^{2n+1}}{(2n+1)!}\right\} + C_0\left(1 - \frac{r^2}{B^2}\right) + \frac{32C_0}{\pi^3}\sum_{m=1}^{\infty}\frac{(-1)^{m+1}}{(2m-1)^3}\left[\cos(2m-1)\frac{\pi r}{2B}\right] \times \left\{\exp -\frac{(2m-1)^2\pi^2 tD}{B^2A} - 1\right\} \quad (17)$$

Along the wake centerline, the mass fraction becomes

$$C(0,t) = \frac{2W_0}{A}\frac{t^{2n+1}}{(2n+1)} + \frac{64W_0(2n)!}{A\pi^3}\sum_{m=1}^{\infty}\frac{(-1)^{m+1}}{(2m-1)^3} \times \left\{\int_0^t \cdots 2n+1 \cdots \int_0^t \exp -\frac{(2m-1)^2\pi^2 tD}{V^2A} \times dt^{2n+1} - \frac{t^{2n+1}}{(2n+1)!}\right\} + C_0 + \frac{32C_0}{\pi^3}\sum_{m=1}^{\infty}\frac{(-1)^{m+1}}{(2m-1)^3} \times \left[\exp -\frac{(2m-1)^2\pi^2 tD}{B^2A} - 1\right] \quad (18)$$

Flat Profiles

If $C_0(r)$ and $g(r)$ are taken as flat, i.e.,

$$C_0(r) = C_0 \quad (19)$$

$$g(r) = 1 \quad (20)$$

Then the solution is

$$C(r,t) = C_0 + \frac{2W_0 t^{2n+1}}{A(2n+1)} \quad (21)$$

This corresponds to a solution neglecting diffusion and radial variations in ion production. The predictions of Eq. (21) agree with those made on a simplified stream-tube analysis, which for the particular reaction to be considered gave as the electron density variation

$$\frac{Ne^-}{P^2} = \left(\frac{Ne^-}{P^2}\right)_I + 4.73(10)^{69}\left(\frac{Px}{U_0/2}\right)^3 \frac{C_{Na}e^{-214,000/T}}{T^7} \quad (22)$$

where T is in degrees Rankine.

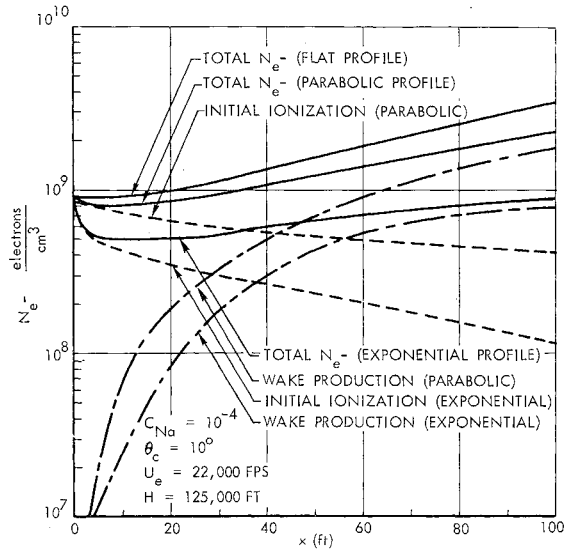

Fig. 1 Sodium ionization at 125,000 ft for various profile shapes.

The preceding results can be nondimensionalized by recognizing that

$$\frac{4Dx^{1/2}}{B^2A} = \frac{d^2}{B^2}\left(\frac{x}{d}\right)^{1/2}\frac{1}{Sc}\left[\frac{3C_D}{2Re_d}\right]^{1/2} \quad (23)$$

Terms associated with C_0 are due to the initial ionization, whereas terms associated with W_0 are due to wake production of ions.

Results

The ionization of sodium by collision with atomic oxygen was considered:

$$Na + 2O \rightarrow Na^+ + e^- + O_2 \quad (24)$$

where the forward rate constant is[4]

$$k = 1.03(10)^{13}\, ft^6\ (\text{lb-mole})^{-2}\ \text{sec}^{-1} \quad (25)$$

The source term for sodium ionization is then described by

$$\frac{\dot{w}}{\rho} = \frac{P^2}{RT^2}C_{Na}\left(\frac{C_O}{M_O}\right)^2 k \quad (26)$$

The source term for production of oxygen atoms is[5]

$$\dot{w}/\rho = 11.6(10)^{16}\,(P/T^2)e^{-107,000/T} \quad (27)$$

Considering the radial temperature profile to be flat near the wake centerline (implying that the centerline oxygen atom mass fraction will be unaffected by diffusion), it follows that the atomic mass fraction is given by

$$C_O = \frac{Px}{U_0/2}\frac{11.6(10)^{16}}{T^2}e^{-107,000/T} \quad (28)$$

Equation (26) can be put into the form of Eq. (10) by substituting for C_O and U_0 from Eqs. (28) and (2), respectively, and by substituting the temperature and pressure of the particular problem. The mass fraction profile of sodium atoms C_{Na} can be represented by any of the functional forms studied. As more significant reactions than (24) are identified, the same type of analysis can be applied.

The sodium ionization predicted by Eqs. (14, 18, and 21 or 22) was studied for a 7-ft, 10° half-angle cone, traveling at 22,000 fps with a wake centerline temperature of 8000°R and a Schmidt number for ambipolar diffusion as 0.5. Two

altitudes were studied: 125,000 ft with a drag D_f of 119 lbf, and 200,000 ft with a drag of 17.4 lbf.

For the exponential profile, B and V were taken to be 0.271, which at the base radius reduces the species values to one percent of their centerline value. For the parabolic, B and V were taken as 1.23, reducing the species to zero at the base radius.

Figure 1 describes the ionization for the various profile shapes. As would be expected, the exponential profile with its sharp peak at the centerline is most reduced by diffusion. The parabolic profile, which might be considered more realistic, shows small reduction due to diffusion at an altitude of 125,000 ft.

Figure 2 describes the ionization predicted for a parabolic profile at 200,000 ft. It is seen that diffusion has a stronger effect at this altitude for the same x, although the stream-tube prediction is still well within an order of magnitude. The fact that diffusion has a larger effect at lower Reynolds numbers could be predicted from Eq. (23) as well as physically

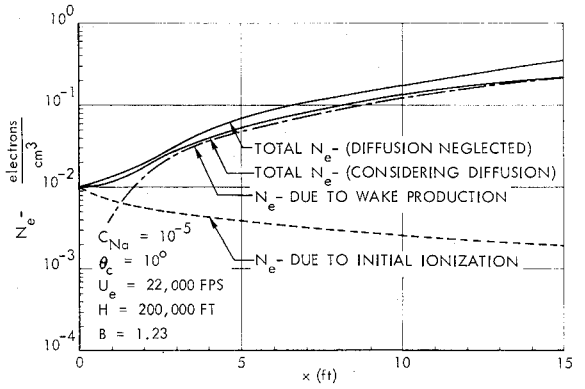

Fig. 2 Sodium ionization at 200,000 ft for parabolic profiles.

anticipated. Figures 1 and 2 describe the breakdown of the ionization into its two components: that due to initial ionization and that due to wake production.

Conclusions

1) The effects of diffusion in laminar hypersonic wakes depend on altitude and specie profile shapes. For parabolic shapes (perhaps physically more reasonable) and for the conditions considered, diffusion has small effect on the centerline electron densities.

2) In contrast to the boundary layer, wake solutions neglecting diffusion [stream-tube or Eq. (21)] are then useful in providing reasonably accurate predictions of contaminated laminar wake ionization if one assumes parabolic radial variations in specie profiles and ion production.

References

[1] Kane, J. J., "Nonequilibrium sodium ionization in laminar boundary layers," AIAA J. 2, 1651–1653 (1964).

[2] Fernandez, F. L. and Levinsky, E. S., "Air ionization in the hypersonic laminar wake of sharp cones," Aerospace Corp., Rept. TDR-269 (S5811-20)-1 (June 1964).

[3] Pallone, A. J., Erdos, J. I., Eckerman, J., and McKay, W., "Hypersonic laminar wakes and transition studies," AIAA Preprint 63-171 (June 1963).

[4] Bortner, M. H., "Chemical kinetics in a re-entry flow field," Space Sciences Lab., General Electric Missile and Space Div., R63SD63 (August 1963).

[5] Levinsky, E. S. and Fernandez, F. L., "Approximate nonequilibrium air ionization in hypersonic flows over sharp cones," Aerospace Corp., Rept. TDR-269 (S4810-60)-1 (November 1963).

Electrical Properties of Rocket Nozzle Boundary Layers

LEROY J. KRZYCKI*
U. S. Naval Ordnance Test Station, China Lake, Calif.

RECENT engineering applications of plasma physics have uncovered several previously unsuspected areas of practical difficulty. This note treats one of these areas, namely, the low level of ionization existing in the boundary layer of partially-ionized gas flows. Magnetogasdynamic (MGD) electrical power generators,[1] MGD accelerators,[2] and magnetotransport experiments[3] have all encountered electrical conductivity problems that can be directly associated with the boundary layer separating the electrode or wall from the core flow. The boundary layer acts like a poor electrical insulator, effectively isolating the partially-ionized core flow from the containment walls.[4]

In support of the experiment discussed in Ref. 3, calculations were undertaken which defined, in the absence of an applied magnetic field, the gas electrical properties in the core and boundary layer of a contoured rocket nozzle. The products of a gaseous oxygen-methyl alcohol combustion process flowed through the nozzle as shown in Fig. 1. The reactants were seeded with cesium carbonate to increase the free electron number density and electrical conductivity of the combustion products.

Calculations

The analysis began with the calculation of the thermodynamic properties of the combustion product gas flowing into the nozzle. Pressure and thermochemical parameters associated with an actual experiment[3] were used as the basis for these calculations. A chemical-equilibrium digital computer program[5] was used to determine the gas temperature, chemical species, other thermodynamic properties, and the free electron number density of the gases in the combustion chamber and the nozzle core flow. The IBM 7094 chemical-equilibrium program considered ionic as well as chemical reactions; the expansion process was based on shifting equilibrium and dissociation of the combustion products. For a combustion pressure of 4.28 atm and an oxidizer-fuel ratio of 1.32 with a seed rate of 4.4% of total flow (by weight), the calculations indicated the stagnation combustion temperature to be 3004°K. On the nozzle core centerline, the static temperature at the geometric sonic throat was calculated at 2873°K, the ratio of specific heats was 1.196, the electron density was 1.39×10^{15} e^-/cm^3, and 0.0269 g-moles of monatomic cesium gas per 100 g of constituents were available for thermal ionization.

The heat transfer through and thickness of the boundary layer on the hot-gas side of the rocket nozzle were calculated using a programed differential equation method, described in Ref. 6. The IBM 7094 program, obtained from Jet Propulsion Laboratory (JPL) and modified by Navel Ordnance Test Station (NOTS), calculated the following as functions of

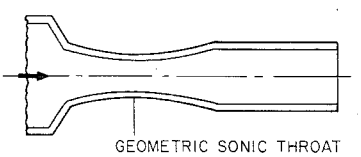

Fig. 1 Contoured convergent-divergent nozzle. Throat diameter is 0.0127 m. Boundary-layer gas-electrical properties discussed in this note were calculated at the geometric sonic throat.

Received October 5, 1964.

* Research Aerospace Engineer, Advanced Technology Division, Propulsion Development Department. Member AIAA.